ISAR for concealed objects imaging

A. Zhuravlev*[a], V. Razevig[a], I.Vasiliev[a], S. Ivashov[a], V. Voronin[b]
[a]Remote Sensing Laboratory, Bauman Moscow State Technical University, 5, 2nd Baumanskaya str., Moscow, Russia 105005; [b]Dept. of Radio-Electronics Systems, Don State Technical University, 1 Gagarina str., Rostov-on-Don, Russia 344010

ABSTRACT

A new promising architecture of microwave personnel screening system is analyzed in this paper with numerical simulations. This architecture is based on the concept of inverse aperture synthesis applied to a naturally moving person. The extent of the synthetic aperture is formed by a stationary vertical linear antenna array and by a length of subject's trajectory as he moves in the vicinity of this antenna array. The coherent radar signal processing is achieved by a synchronous 3D video-sensor whose data are used to track the subject. The advantages of the proposed system architecture over currently existing systems are analyzed. Synthesized radar images are obtained by numerical simulations with a human torso model with concealed objects. Various aspects of the system architecture are considered, including: advantages of using sparse antenna arrays to decrease the number of antenna elements, the influence of positioning errors of body surface due to outer clothing. It was shown that detailed radar images of concealed objects can be obtained with a narrow-band signal due to the depth information available from the 3D video sensor. The considered ISAR architecture is considered perspective to be used on infrastructure objects owing to its superior qualities: highest throughput, small footprint, simple design of the radar sub-system, non-required co-operation of the subject.

Keywords: microwave imaging, radar imaging, sparse array, synthetic aperture radar, concealed weapon detection, personnel screening, infrastructure security, transport security.

1. INTRODUCTION

In recent years active microwave body scanners have taken their steady place in the global market. The primary radar image generated in those systems is the result of processing the scattered microwave field acquired on a discreet sampling points distributed over a limited surface area in the vicinity of the subject. These systems can be formally divided into two categories: the systems that use mechanical scanning to form a synthetic aperture and motion-free systems with distributed electronically switched (or steered) antenna elements with digital beamforming. The radar signal processing in both categories happens under assumption that the inspected subject is stationary during a scan cycle, which takes, on the orders of magnitude, one second in the systems with mechanical scanning, and one tenth of a second in the systems with electronic switching. The systems that steered electronically are more tolerant to movements of the subjects as the sampling cycle is much shorter than that of the systems with mechanical scanning.

A distinct representative of a microwave screening system that uses mechanical scanning is L-3 ProVision [1]. The system uses two linear arrays of antenna elements that move around the subject to acquire the radar samples over a cylindrical aperture. Other systems that employ fully electronic control of spatially distributed antenna elements without mechanical movements include Eqo by Smiths Detection [2] and QPS by Rohde&Schwarz [3]. The latter two systems exhibit a common approach toward decreasing their footprints by distributing antenna elements over a flat panel rather than creating a portal to isolate the area where linear antenna arrays move.

Multi-side images in L-3 ProVision are obtained by illuminating the subject from all directions due to mechanical movement of the linear antenna arrays around the subject, while obtaining radar images with a flat panel requires subject's self-rotation to get at least two images of his front and back sides. For this reason, the throughput of the systems that have one panel with antenna elements must be comparable to the throughput of the systems with mechanical scanning because of this self-rotation, which, in average, must take longer than predefined movement of a mechanical part (the scan time in L-3 ProVision equals to 1.5 seconds according to [1]).

*azhuravlev@rslab.ru; phone/fax 7 495 632-2219; rslab.ru

Computational Imaging XIII, edited by Charles A. Bouman, Ken D. Sauer, Proc. of SPIE-IS&T Electronic Imaging, SPIE Vol. 9401, 94010I · © 2015 SPIE-IS&T
CCC code: 0277-786X/15/$18 · doi: 10.1117/12.2081761

The capability of generating radar images at video rates in one-panel real-time systems, due to current advances in electronics, does not help increasing the throughput of a single unit, estimated for L-3 ProVision at 200-300 people per hour. The systems are targeted to deploy in airports and other critical infrastructure objects where combination of their throughput and price meets the requirement to screen every passenger, employee, or visitor.

The following parameters of currently deployed active microwave screening systems limit their wider deployment in other places where a higher level of security is desirable: high price, limited throughput, large mass and footprint, requirement for the subject to co-operate during the screening process. Among the approaches to improve these and other parameters the following can be mentioned.

Decreasing the price of the system can be achieved by reducing the number of expensive microwave components, including antennas and other relevant circuitry. One approach to reducing the number of antenna elements is to employ mechanical scanning, which increases the number of spatially distributed signal samples without increasing the number of antenna elements. For example, scanning on a cylindrical aperture is used in L-3 ProVision.

Another approach to reducing the number of antenna elements is to use a multiple input – multiple output antenna (MIMO) configuration [4, 5]. In a MIMO radar system the same volume of independent samples is achieved by a lesser number of antenna elements than in a classical radar system. This comes from the fact that in a MIMO radar system each transmitter operates with each receiver while in a classical radar system each antenna element is a transceiver, or each transmitter operates with a fixed relevant receiver.

An interesting approach, which stays within the modern trend of complete electronic scanning, to increasing the throughput of a microwave body screening system was demonstrated by Camero [6] at the VII Integrated Safety and Security Exhibition, held in Moscow, 20-23 May 2014. The presented microwave screening system of Camero is a portal that has cylindrical shape with octagon at its base. Two opposite faces of that octagon serve as the entrance to and the exit from the portal, while other six facets are formed by flat panels with multiple antenna elements [7, 8]. The antenna elements of the system are steered electronically to generate approximately a dozen frames per second. Multi-side views of the subject are obtained due to arranging the panels with antenna elements from all sides to the subject. The portal of the system is not transparent for the operator to see the subject because its walls host panels with antenna elements. A video camera inside the portal is used to provide video of the subject to the operator of the system. Thereby, increasing the throughput by obtaining simultaneously multi-sided views at the expense of multiple antenna panels does not decrease the complexity of the microwave hardware nor the mass or footprint of the system.

Mechanical scanning with a dense or sparse antenna array, or applying one or many panels with antenna elements distributed in two dimensions to eliminate that mechanical scanning may still leave one possibility to designing a competitive, lightweight, compact, and cheap microwave screening system with high throughput. Such architecture of a microwave screening system is analyzed in this article. The considered approach relies on the concept of inverse aperture synthesis, when the subject moves in the vicinity of a stationary distributed and vertically arranged antenna elements. The subject can move naturally by the antenna system without a treadmill or other transport tool and this natural arbitrary movement is used to form a synthetic aperture and, eventually, to calculate a detailed radar image.

2. MICROWAVE SCREENING SYSTEM OF INVERSE SYNTHETIC APERTURE

Traditionally, the concept of inverse synthetic aperture is applied to air or naval targets, which have six degrees of freedom: three rotation angles and three coordinates of a selected point that belong to this target [9]. Special techniques exist to evaluate these parameters and generate radar images with spatial resolution that is high enough to reveal the structure within the size of the target. This technique can not be applied directly to a walking person because the shape of the person changes continuously while moving, and the six parameters are definitely not enough to characterize the moving person to get the radar images which are as detailed as those obtained in modern microwave screening systems obtained with a static person. The formulated problem seems unsolvable due to the arbitrary movement of the person while walking and the large number of degrees of freedom associated with the human body. However, the advances of modern technology of three-dimensional capture of the observed dynamic scene, including moving humans, allow formulating the approach to obtaining detailed radar images in a microwave screening system of inverse synthetic aperture.

In [10], authors of this paper gave a concept of a microwave screening system of inverse aperture synthesis on the basis of the radar system with distributed antenna elements and a synchronous 3D video sensor like time-of-flight camera

(TOF-camera) or other. The output data of such a sensor are streams of gray scale or RGB images, each pixel of which has an additional attribute of depth. In TOF-cameras the depth is obtained by measuring the time of flight for the light emitted by the active element of the camera and received by a special CCD-matrix. Each cell of this matrix measures the time of flight independently [11]. Modern cameras are capable of measuring distance for each pixel with absolute error of 1 cm and resolution of 640 by 480 pixels or higher. The operation distance varies from tens of centimeters to a few kilometers [12]. The synthetic radar image in a radar system with inverse synthetic aperture can be obtained with the same resolution provided by the video sensor, because this resolution defines the minimal size of a region on the optical image. Each such pixel may become a "focusing point" when processing the synchronously registered radar signal. For this purpose it must be tracked independently, or in a relationship with other adjacent pixels.

When the subject moves past a stationary antenna system consisting of multiple distributed antenna elements, the coherent radar signal processing requires that trajectories of body surface and that of clothing are extracted. There exist numerous approaches to this problem in computer vision, including parametric models that describe realistically the human body [13-15]. The synthesized radar image would result from focusing the radar signal into each node of the grid that is given by the models of the human body and the clothing. The surfaces of the human body and the clothing could be considered separately if subjects in heavy outer clothing to be inspected. The result of processing the radar signal with the known trajectory of the human body should be similar to the result obtained with a static subject and mechanical scanning. Knowing the trajectory of the human body surface gives possibility of synthesizing the radar image for an arbitrary pose of the moving subject. Calculating the radar image for the pose in each video frame of the 3D-sensor will result in generating a video stream of radar images. This video stream can be generated with a time lag required to record a sufficiently long trajectory, or, by other words, after sufficiently long inverse aperture was achieved in the horizontal direction. The length of this trajectory should be comparable to the size of the portal of modern microwave screening system, or the length of a panel of the systems with electronic steering if comparable resolution is expected.

A possible geometry of the proposed microwave screening system is shown in Figure 1. The system has two linear vertically oriented antenna arrays placed from both sides of the subject to be examined. The linear arrays form gates through which the subject should move. The architecture of the linear antenna arrays may be based on dense or sparse (MIMO) sampling technique. One or more 3D video sensors are used to capture the motion of the subject as he moves through the gates. The radar system and the video sensors must be synchronized to get the signal that corresponds to the same instant pose of the subject. The directivity diagram of the individual antenna elements should be wide enough to illuminate the whole subject's body. The interference from foreign objects in the vicinity of the moving subject can be reduced by electronically steered antenna diagram that follows the subject (spotlight ISAR). Increasing the effective synthetic aperture in horizontal direction is another benefit of applying spotlight ISAR, which should allow obtaining detailed radar images of front and back sides of the subject.

One concern of this article is to study, by numerical simulation, the possibility of obtaining multi-view synthesized radar images in the geometry shown in Figure 1, when the subject moves between linear vertical antenna arrays. The compact size of the microwave screening system in this case would allow its design in a form of a metal detector frame, gates, or, possibly, a concealed implementation to install in doorways.

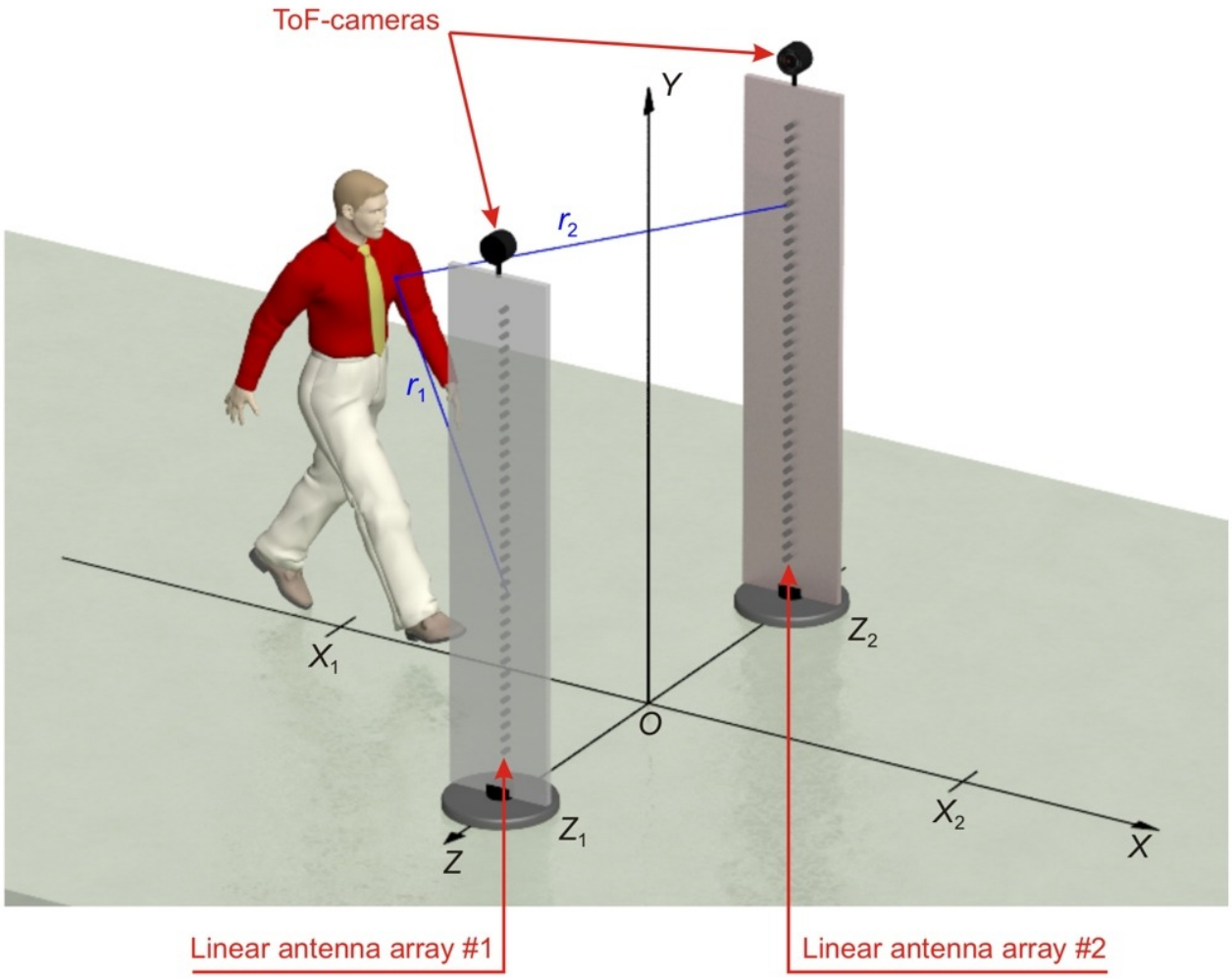

Figure 1. A possible geometry of the microwave screening system implemented as ISAR.

3. MATHEMATICAL MODEL OF RECEIVED SIGNAL

Calculations were performed with a 3D model of a human torso and an attached foreign object with a silhouette of a pistol as it shown in Figure 2. The full body was not considered to decrease computational time and to focus on principal effects that influence the reconstruction of radar images obtained for an arbitrary moving subject. By calculating the scattered field the torso was considered as a dense grid of point scatterers that cover it densely between the vertexes that describe the geometry of the torso [16].

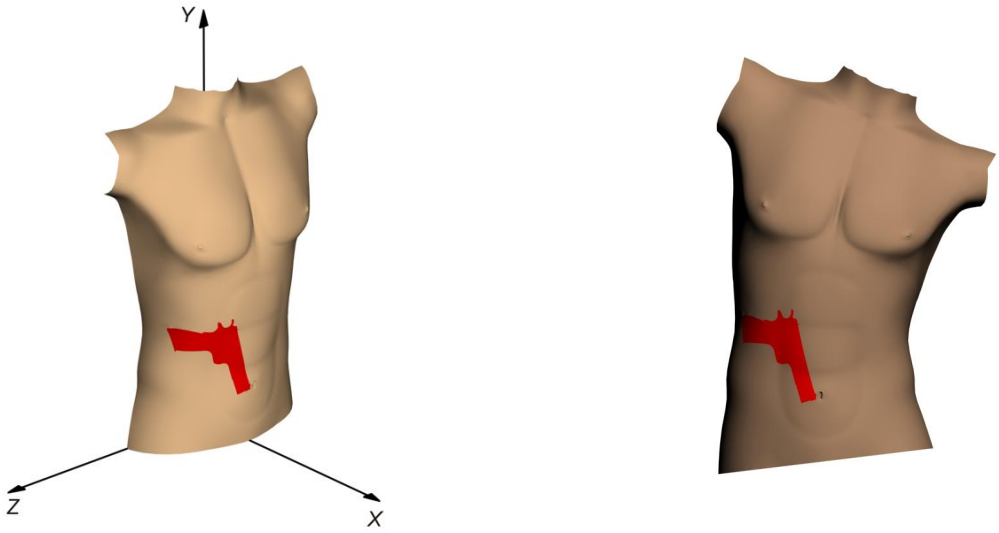

Figure 2. The model of an animated human torso with a foreign object used in the simulations: the torso model (left), the same torso with a bend (right).

Two types of linear antenna arrays situated at both sides from the walking subject were considered: the first antenna array implemented dense sampling and consisted of transceivers separated at fractions of a wavelength, the second type of antenna array was a MIMO system. The numbers of antenna elements in both types of antenna arrays were chosen to give approximately the equal numbers of effective samples of the radar signal.

In the case with dense sampling, the complex amplitude of the signal registered the receiver in the receiver-transmitter pair with index n, transmitter coordinate vector $\mathbf{r}_n^{Tx}$ and receiver coordinate vector $\mathbf{r}_n^{Rx}$ at time t on frequency f is given by

$$E(n,t,f)=\sum_{j=1}^{K}\left[\frac{\sigma_j}{\left|\mathbf{r}_n^{Tx}-\mathbf{r}_j(t)\right|\cdot\left|\mathbf{r}_n^{Rx}-\mathbf{r}_j(t)\right|}\cdot\exp\left(i\cdot\frac{2\pi f}{c}\cdot\left(\left|\mathbf{r}_n^{Tx}-\mathbf{r}_j(t)\right|+\left|\mathbf{r}_n^{Rx}-\mathbf{r}_j(t)\right|\right)\right)\right], \quad (1)$$

where K is the number of point scatterers approximating the object; $\mathbf{r}_j(t)$ — coordinate vector of scatterer j at time t; c — the speed of light; σ_j — effective scattering area (reflectivity coefficient) of scatterer j. The directivity diagram of antennas was not taken into account.

The registration of the signal starts at t_1 when the subject has coordinate x_1 and stops at t_2 when the subject reaches coordinate x_1.

In the case with a MIMO antenna array the complex amplitude of the signal registered by the receiver with index m and coordinate vector $\mathbf{r}_n^{Rx}$ from the transmitter with index n and coordinate vector $\mathbf{r}_n^{Tx}$ at time t on frequency f is given by

$$E(n,m,t,f)=\sum_{j=1}^{K}\left[\frac{\sigma_j}{\left|\mathbf{r}_n^{Tx}-\mathbf{r}_j(t)\right|\cdot\left|\mathbf{r}_m^{Rx}-\mathbf{r}_j(t)\right|}\cdot\exp\left(i\cdot\frac{2\pi f}{c}\cdot\left(\left|\mathbf{r}_n^{Tx}-\mathbf{r}_j(t)\right|+\left|\mathbf{r}_m^{Rx}-\mathbf{r}_j(t)\right|\right)\right)\right], \quad (2)$$

where all other variables are the same as in Equation 1.

4. RADAR IMAGE SYNTHESIS

Obtaining radar images in the modern active microwave screening systems involves calculating a function that characterizes radar reflectivity for a definite volume occupied by the subject. This stage is computationally intensive and requires special hardware in the systems that generate radar images at video rates. Eventually, the radar image is obtained by visualizing this pre-calculated volume of data.

The radar system considered in this article is based on a 3D video sensor that sees and tracks the subject. In this situation, the calculations should be made only for a reduced number of points that belong to the surface of the subject, not the volume where the subject is expected to be. Another advantage of the considered radar system related to computational aspect is more relaxed requirements to the computing power of radar data processor. This comes from the fact that the radar data are acquired gradually as the subject moves through the sensitive area of the system to form a sufficiently long inverse aperture. These data can be processed as soon as they available. Thus, the total volume of radar data, which substantially smaller compared to the modern radar systems, is to be processed during the time when the subject moves through the screening system.

The data stream of the 3D video sensor, the radar data processing here is based on, consists of grayscale or RGB images with each pixel having an additional depth attribute. Extracting the motion of the body surface requires that the model representation of that surface exists that gives extrapolation of the body surface and the surface of outer clothing (to image any concealed objects attached to it). The input data to this model can be observable features, based on intensity, depth data, or both, as they used in computer vision. The 3D sensor data processing required here may be based on the approaches of extracting the model parameters of human body representation with description of that model [13-15].

In this work, the problem of finding the body surface trajectory by processing 3D sensor data was not considered. Instead of it, the tracking of the body surface was based on known geometric representation of the subject according to the following:

- The shape of the human torso used in the simulations was given by the corresponding facet model (Figure 2)
- The motion of the torso was performed in 3ds Max [17] by creating an animation sequence that mimicked the motion of human torso while walking
- For each animation frame the vertexes of all facets were remembered individually
- Using an arbitrary frame (the key frame) with a desired pose, a dense grid to be used for calculating the radar image was generated for each facet according to the approach given in [16]
- Affine transform matrices for all facets were calculated under assumption that the correspondence between vertexes of the object on the key frame and any other frame in the sequence is known
- The trajectory of the whole body surface was found by applying a relevant affine transform, calculated for a facet vertexes, to the nodes of the dense grid belonging to this facet

The radar images were obtained using the back projection algorithm [18]. In the dense sampling case the reconstructed reflectivity function corresponding to point j with coordinate vector $\mathbf{r}_j(t_1)$ belonging to the surface of the subject is given by

$$S\left(\mathbf{r}_j(t_1)\right) = \sum_{t=t_1}^{t_2}\sum_{n=1}^{N}\sum_{f=f_{\min}}^{f_{\max}}\left[E(n,t,f)\cdot\exp\left(-i\cdot\frac{2\pi f}{c}\cdot\left(\left|\mathbf{r}_n^{Tx}-F_j(t)[\mathbf{r}_j(t_1)]\right|+\left|\mathbf{r}_n^{Rx}-F_j(t)[\mathbf{r}_j(t_1)]\right|\right)\right)\right], \quad (3)$$

where N is the number of transceivers; $E(n,t,f)$ — the complex amplitude of the received signal on frequency f; $\mathbf{r}_j(t_1)$ — coordinate vector of node j on the dense grid of the reflecting object at time t_1; $F_j(t)$ — the affine transform that maps node j from the position at time t_1 to the position at time t; $\mathbf{r}_n^{Tx}$, $\mathbf{r}_n^{Rx}$ — the coordinate vectors of the transmitter and the receiver with index n; f_{min}, f_{max} — minimal and maximal frequencies of the radar signal; t_1, t_2 — the first and the last moments of the signal time interval.

In the case with a MIMO antenna array the formula for reflectivity function is given by

$$S\left(\mathbf{r}_j(t_1)\right) = \sum_{t=t_1}^{t_2}\sum_{n=1}^{N_{Tx}}\sum_{m=1}^{N_{Rx}}\sum_{f=f_{\min}}^{f_{\max}}\left[E(n,m,t,f)\cdot\exp\left(-i\cdot\frac{2\pi f}{c}\cdot\left(\left|\mathbf{r}_n^{Tx}-F_j(t)\mathbf{r}_j(t_1)\right|+\left|\mathbf{r}_m^{Rx}-F_j(t)\mathbf{r}_j(t_1)\right|\right)\right)\right], \quad (4)$$

where N_{Tx}, N_{Rx} — the numbers of transmitters and receivers respectively; $E(n,t,f)$ — the complex amplitude of the signal received by receiver m from transmitter n on frequency f; all other variables correspond to Equation 3.

Obtaining a radar image is the result of applying one of the above formulas to every node of the dense grid that approximate the surface of the subject, which is followed by projecting the result to a desired plane.

5. SIMULATION RESULTS

5.1 Reconstruction of radar images at walking

The trajectory of the torso at walking was generated with a tool available in 3ds Max to render realistic motion of the human body. The walking speed was taken equal to 1 meter per second; the sampling frequency of the radar signal was equal to 50 Hz; the 3D images of the scene were available with the same rate as the sampling frequency of the radar signal. In addition to the forward motion along axis X (Figure 1) the torso had periodical movements along axes Y and Z accompanied by a slight rotation along axis Y and a slight motion in the opposite direction of axis Z. The trajectory is shown in Figure 3.

The simulation with a moving torso was done for linear antenna arrays with 200 transceivers spaced at intervals of 2 cm. The distance between the antenna arrays was equal to 1 m with their coordinates z_1=0.5 m, z_2=0.5 m, in the geometry shown in Figure 1. The acquisition of the signal started from the mark x_1= -2 m and stopped at x=0 m, giving the size of synthetic aperture of 2 m. The minimal and maximal frequencies of the stepped-frequency radar signal were equal to 10 and 16 GHz correspondingly with the frequency step Δf=0.5 GHz.

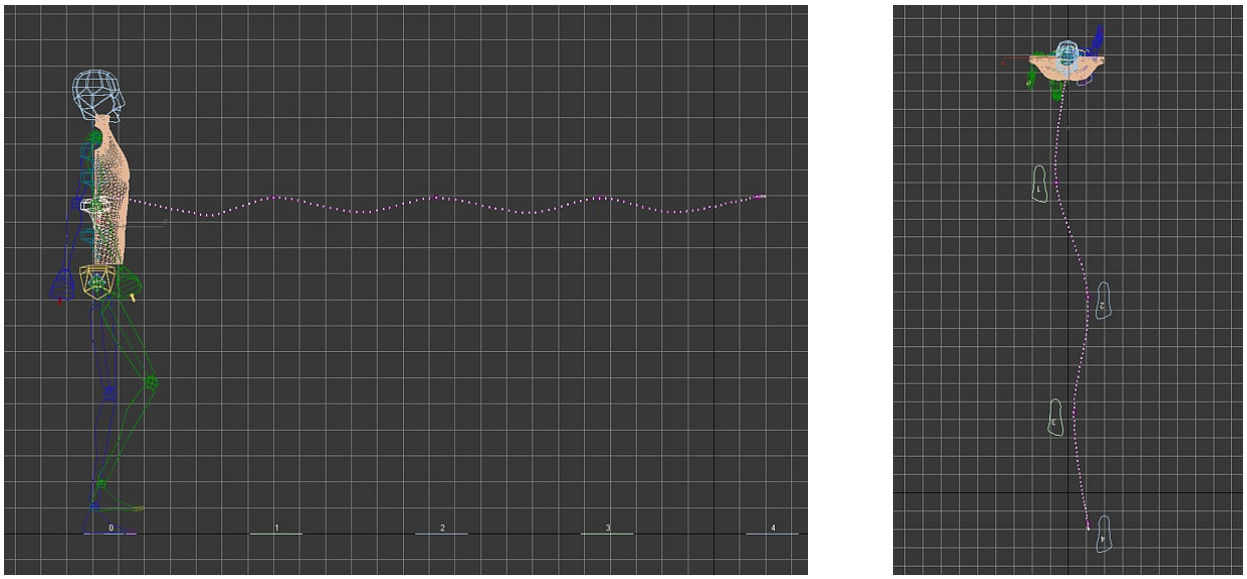

Figure 3. The trajectory of the torso used in the simulation: right side view (left picture), top view (right picture).

The radar images were obtained by the technique described in the previous section. The first frame of the generated video sequence was used as the key frame. The radar image was visualized by projecting it to plane YOZ with resampling to a grid with the steps of 5 mm along axes Y and Z. The reconstructed radar image has size 0.5 by 0.7 meters and it is shown in Figure 4 on the left. To generate the demonstrated radar image the signal only from the antenna array on the right side of the torso was considered, which explains why one side of the torso is brighter than the other. All other radar images to follow are also obtained by processing the signal from the antenna array situated on the side of the torso that has a foreign object.

The radar image calculated without precise trajectory information, suggesting that the torso moves strictly along axis X, is shown in the same figure on the right. It is seen that a rough estimation of the trajectory makes radar image reconstruction impossible. An important question that is addressed in one of the following sections is estimating tolerable errors in positioning precision.

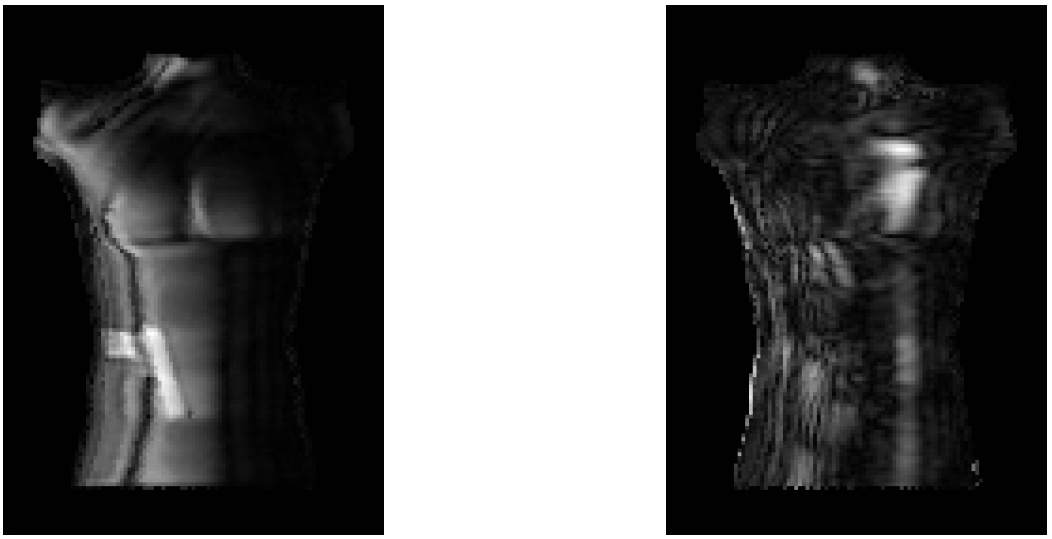

Figure 4. Calculating the radar image: with precise trajectory information available (left), with a rough estimation of the trajectory (right).

The influence of human body flexibility on reconstruction of radar images was also considered in a simulation where the torso with an attached object bends from its original shape shown in Figure 2 on the left to the pose shown in the right while moving uniformly along axis *X*. It was mentioned already on the possibility of using an arbitrary pose as the base for the radar image. In the simulation with a bending torso the reconstruction of radar images was done for the initial and final poses of the torso. The corresponding result is shown in Figure 5, where any changes in the image of the foreign object are substantially small. It is seen from the demonstrated radar images in Figure 4 that knowing the motion of the surface allows obtaining clear radar images.

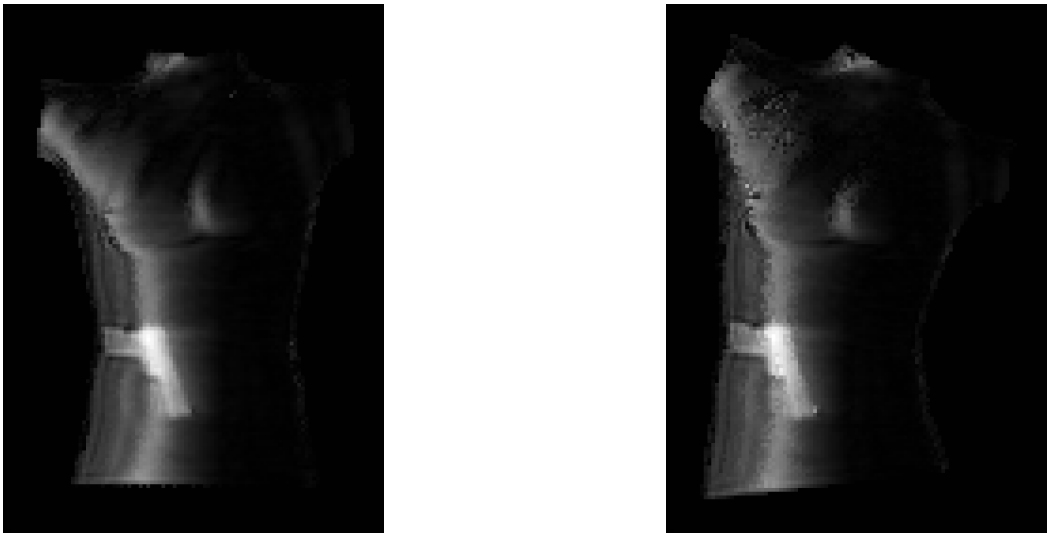

Figure 5. The reconstructed radar images corresponding to the initial and final poses of a bending torso.

5.2 Dense array versus sparse array

The comparison of the two types of antenna arrays was done with the parameters given in Table 1. The number of transmitters and receivers in the sparse antenna array were chosen to meet approximately equation $N_{Tx}N_{Rx} = N$ that expresses equality of total samples of the signal in the antenna arrays in terms of Equations 3 and 4. The solution gives the numbers N_{Tx}=14, N_{Rx}=15 with 210 effective samples on a single frequency. The spacing between antenna elements in

the sparse antenna array was chosen according to the technique given in [4] minimizing the level of side interference lobes of the antenna system. The spacing of receivers in the sparse antenna array was chosen larger than that of the transmitters to form sufficiently extent vertical aperture. The size of synthetic aperture in Table 1 implies that the signal was recorded starting from the mark x_1=-2 m to x=0 m.

Table 1. Parameters used in the simulation to compare dense and sparse linear antenna arrays.

		Dense antenna array	Sparse antenna array
Type of antenna array		Linear equidistant antenna array	
Number of transmitters		-	14
Number of receivers		-	15
Number of transceivers		200	-
The intervals between adjacent:	transmitters, cm	-	2.2
	receivers, cm	-	14
	transceivers, cm	1	
Minimal frequency, GHz		10	
Maximal frequency, GHz		16	
Frequency step, GHz		0.5	
Number of discrete frequencies		13	
The size of synthetic aperture along axis X, m		2	
Sampling rate, Hz		100	
Object trajectory type		Linear translation along axis X	
Object's speed, m/s		1	
The distance between antenna arrays, m		1	

The radar images synthesized for both cases are shown in Figure 6. The benefits of applying sparse antenna arrays become evident: radar images of the same quality can be obtained by substantially lesser number of antenna elements. In the specified conditions the reduction by a factor of 7 is achieved if transceivers are used in the dense antenna array. If the dense antenna array consists of separate transmitters and receivers then the reduction factor doubles to 14.

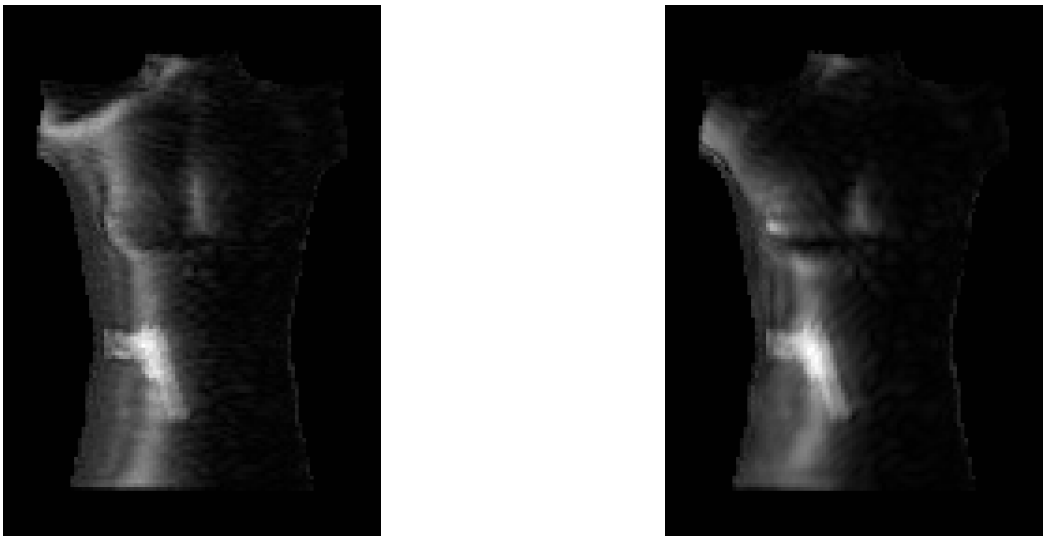

Figure 6. Radar images obtained with dense antenna array (left) and sparse antenna array (right). Sparse antenna array has reduced number of antenna elements by a factor of 7.

It is interesting to observe that even further decrease in the number of antenna elements in the sparse antenna array still allows obtaining radar images with a recognizable foreign object. The considered variants of sparse antenna arrays are enumerated in Table 2 with other varying parameters given.

Table 2. Sparse antenna array variants.

Case	N_{Tx}	N_{Rx}	Tx step, cm	Rx step, cm
1	14	15	2.2	14.0
2	10	10	4.9	22.0
3	8	8	8.2	28.6
4	7	7	11.3	33.4
5	6	6	16.0	40.0

The radar images corresponding to the cases from Table 2 are shown in Figure 7.

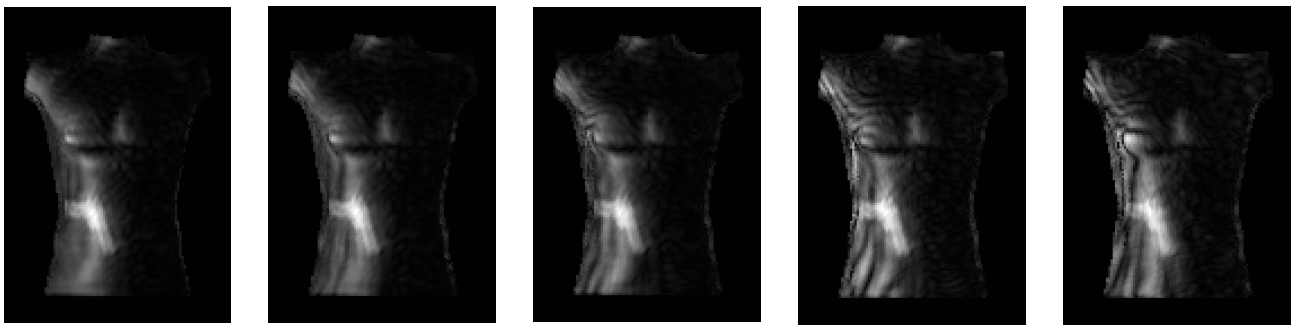

1 2 3 4 5

Figure 7. Radar images obtained for the sparse antenna arrays having various numbers of transmitters and receivers.

Application of sparse antenna arrays may substantially reduce the number of antenna elements without sacrificing the quality of the radar image. The proposed technique of inverse aperture synthesis pushes the reduction factor to the limit

because the number of antenna elements may be reduced to a couple of dozens from several hundreds or thousands that are found in modern electronically steered systems.

5.3 Influence of the synthetic aperture length

The approach considered in this paper uses natural motion of the subject to form a synthetic aperture rather then the motion of an antenna array in the vicinity of the subject. The parameter that influences the resolution of obtained radar images is the length of the synthetic aperture (absolute value of x_1 in Figure 1) for which the radar signal must be accumulated and processed. To estimate the influence of synthetic aperture size in the direction of axis X, a series of radar images was calculated corresponding to the following lengths of synthetic aperture: 1, 1.5, and 2 meters (the corresponding starting point of the subject x_1=-1, -1.5, -2 m). The radar images calculated for these lengths are shown in Figure 8.

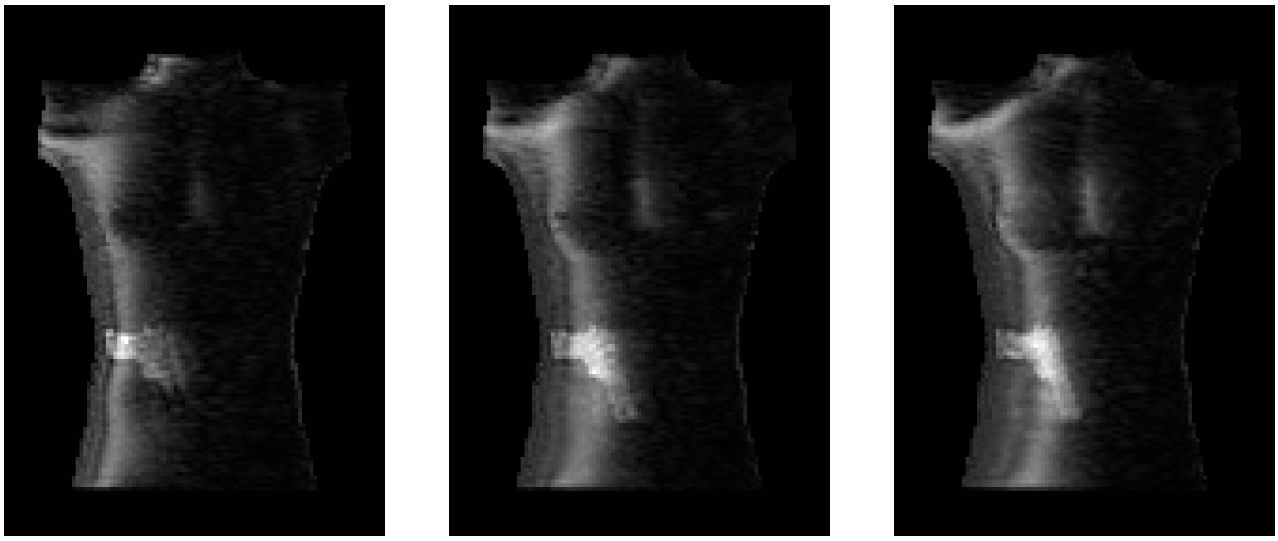

Figure 8. Radar images calculated for the different lengths of synthetic aperture: 1 m (left), 1.5 m (middle), 2 m (right).

The images given in Figure 7 suggest that for the considered geometry the radar signal acquisition should start not less than from 1.5 meter away from the antenna array when the subject approaches the antenna arrays. The same distance must be provided to acquire the signal from the back side of the subject.

5.4 Influence of clothing

The technique of calculating the radar images of animated objects with inverse aperture synthetic relies on the data provided by a synchronous 3D video sensor that captures the depth map of the scene. The depth map of a dressed subject gives the surface of the outer clothing while the radar signal processing requires the knowledge of the body surface. This should influence the choice of antenna array, its geometry, and signal parameters. To estimate the influence of clothing on the synthesized radar images, simulations were done with the dressed torso and foreign objects shown in Figure 9. In these simulations the depth map was calculated for the dressed torso, while the received radar signal was calculated for the torso model with a foreign object. At the reconstruction stage, the trajectory of the dressed torso was used.

The following considerations were guiding the choice of the foreign objects. A foreign flat object visible in Image A in Figure 9 follows the body surface. Two times higher reflectivity of the object compared to the torso is taken and designated by foreign object's red color. It can only be revealed by reflectivity contrast in radar images. The reflectivity of the foreign object in Image B is the same as that of the torso. It stands out for about 2 cm from the torso surface and introduced to estimate the influence of the signal bandwidth on the depth resolution. Image C is the combination of the two cases where the foreign object both stands out and has twice as high reflectivity as that of the torso.

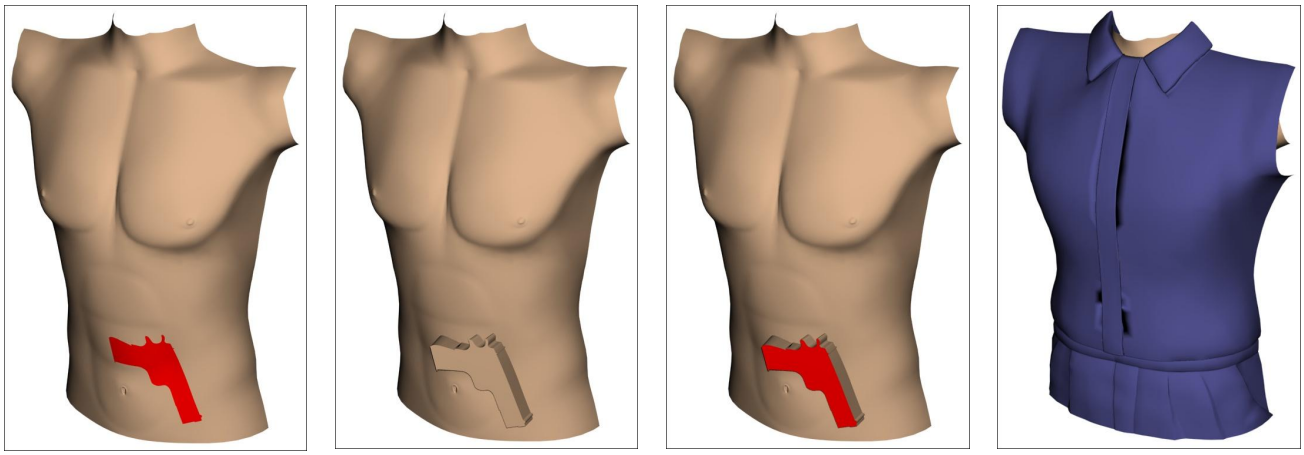

A B C D

Figure 9. Different concealed objects used in simulations with a dressed torso. A twice higher reflectivity of foreign objects is highlighted by red.

The radar images for concealed objects A, B, and C, placed under the clothing in Image D, were obtained for the dense antenna array with corresponding parameters given in Table 1 (further referred to as the wide-band case). A single-frequency case was also considered where processing of the radar signal was done only on the frequency of 16 GHz (further referred to as the single-frequency case) with other parameters as in the multi-frequency case.

Figure 10 shows the radar images reconstructed for the surface of the torso. All foreign objects are revealed as it expected to be due to precise knowledge of the body surface. The letters under the radar images shown in Figure 10 correspond to the letters that designate foreign object in Figure 9.

Figure 11 and 12 show the radar images reconstructed for the clothing surface for the wide-band and the single-frequency cases. By comparing the obtained radar images the following conclusions can be made. The error of positioning of about 2 cm prevents revealing the foreign object in the radar image for the case A. The pistol silhouettes in the radar images for the cases B and C are observable due to close proximity of the object to the outer surface of the clothing. The distance between the outer surface of the concealed object and the surface of the clothing is smaller than 2 cm and both surfaces belong to the same resolution cell. Revealing the object in this case would require synthesizing a series of radar images that span a layer from the observable surface of the clothing to the surface of the torso. One option is using a better approximation of the torso surface based on the observable surface of the clothing. Figure 12 supports the idea of extending the focusing depth by diminishing bandwidth of the radar signal as the foreign object is distinguished in all radar images.

This possibility of using a single frequency to obtain radar images of a concealed object when the distance to the surface is known within a relatively small error seems attractive to test in a real experiment because positive results would suggest that obtaining detailed radar images of concealed objects is possible with a single frequency or a narrow-band signal. The radar system then may be designed on the basis of planar structures, which may prove beneficial both for SAR- and ISAR-based people screening systems.

A B C

Figure 10. The radar images obtained with precise knowledge of the surface. The wide-band case.

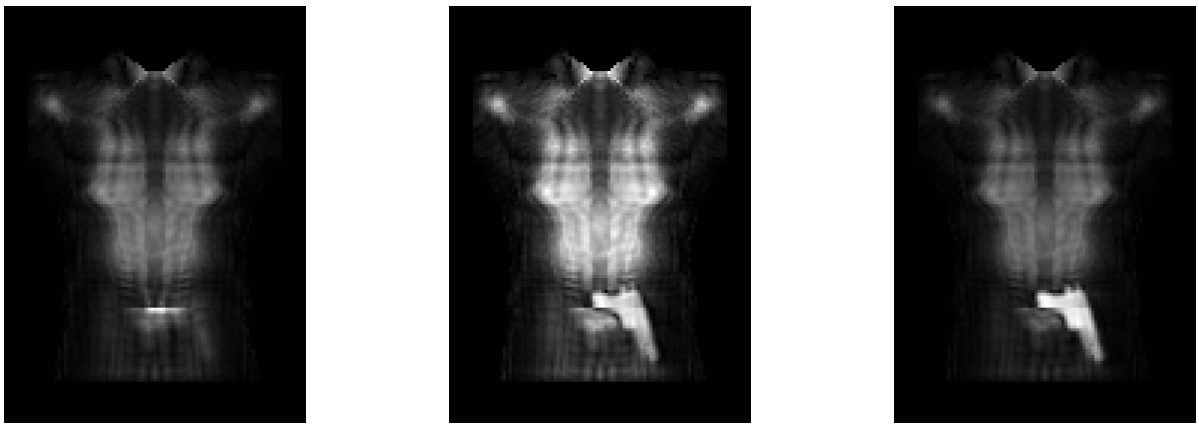

A B C

Figure 11. The radar images obtained by using the surface of the clothing. The wide-band case.

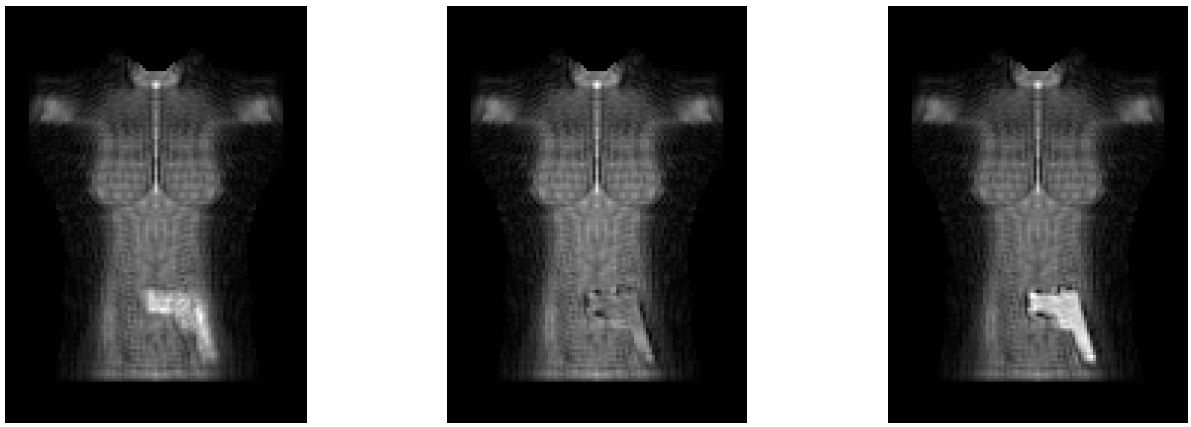

A B C

Figure 12. The radar images obtained by using the surface of the clothing. The single-frequency case.

6. CONCLUSION AND FUTURE WORK

The results obtained in this paper support the idea of using the principle of inverse aperture synthesis in a microwave screening system resulting in a number of advantages in comparison to the modern microwave screening systems. The highest possible throughput may be achieved due to the main principle of the considered system: the requirement to walk past a linear antenna arrays instead of moving the antenna array around a stationary subject. Sufficiency of using only linear antenna arrays, rather than modern massive two-dimensional antenna arrays, allows the system to be compact and, if required, mobile. Co-operation of the subject is not required as an arbitrary movement of the subject, as he walks through the system, is tracked by a 3D video sensor. It is these data that allow coherent radar processing of a moving animate subject. Using sparse antenna arrays may substantially reduce the complexity of the microwave part of the system. One possible implementation of the considered system may use a single-frequency or narrow-band signal to rely on the range data provided by the 3D video sensor. It was shown in this paper that such "downgrade" of the radar system may simplify radar signal processing while still obtaining detailed radar images. Moreover, in this case, a design of the system may rely on planar technology and use cheap narrow-band microwave components. The considered system does not require high-performance data processor because the data stream is generated by a small number of antenna elements and the radar image must be calculated for a smaller number of points during the time that is required to cross the screening system, not during the time that inversely proportional to a desired frame rate as it is in the modern electronically steered systems.

The formulated concepts will be tested in an experimental setup to be made during the further development of the project. It is planned to obtain experimental radar images and estimate all considered here possibilities of radar system design, including dense and sparse antenna arrays as well as possibility of using a single-frequency or narrow-band signal.

ACKNOWLEDGEMENT

This work is supported by the Ministry of Education and Science of the Russian Federation.

REFERENCES

[1] "ProVision® Imaging," 2014, <http://www.sds.l-3com.com/advancedimaging/provision.htm> (15 January 2015).
[2] "eqo," 3 June 2013, <http://www.smithsdetection.com/index.php/en/products-solutions/people-screening-systems/60-people-screening-systems/eqo.html> (15 January 2015).
[3] Ahmed, S. S., "Personnel screening with advanced multistatic imaging technology," Proc. of SPIE 8715, (2013).
[4] Razevig, V. V., Bugaev, A. S., Chapursky, V. V., "The comparative analysis of classical and multistatic microwave holograms focusing," Radiotekhnika 8, 8-17 (2013) (in Russian).
[5] Sheen, D. M., Hall, T. E., "Reconstruction techniques for sparse multi-static linear array microwave imaging," Proc. of SPIE 9078, (2014).
[6] <http://www.camero-tech.com> (15 January 2015).
[7] Sherbin, B., "GPU startup story: Camero goes beyond seeing through walls to real-time body scanning," 30 October 2012, <http://blogs.nvidia.com/blog/2012/10/30/gpu-startup-story-camero-goes-beyond-seeing-through-walls-to-real-time-body-scanning/> (15 January 2015).
[8] Beeri, A., Daisy, R., "System and method for volume visualization in ultra-wideband radar imaging system," US Patent #2014/0055297 A1.
[9] Skolnik, M. I., [Introduction to Radar Systems], Tata McGraw Hill (2003).
[10] Zhuravlev, A., Ivashov, S., Razevig, V., Vasiliev, I. and Bechtel, T., " Inverse synthetic aperture radar imaging for concealed object detection on a naturally walking person," Proc. of SPIE 9074, (2014).
[11] Li, L., "Time-of-Flight Camera – An Introduction," Technical White Paper, May 2014, <http://www.ti.com/lit/wp/sloa190b/sloa190b.pdf> (15 January 2015).

[12] Stettner, R., "3D Flash LIDAR Cameras™ For OOS Applications," 26 March 2010, <http://ssco.gsfc.nasa.gov/workshop_2010/day3/Roger_Stettner/Stettner_ASC_Workshop_Presentation.pdf> (15 January 2015).
[13] Anguelov, D., Srinivasan, P., Koller, D., Thrun, S., Rogers, J. and Davis, J., "SCAPE: Shape Completion and Animation of People," Journal ACM Transactions on Graphics (TOG) - Proceedings of ACM SIGGRAPH 2005 24(3), 408-416 (2005).
[14] Kasap, M., Magnenat-Thalmann, N., "Parameterized Human Body Model for Real-Time Applications," International Conference on Cyberworlds, 160-167 (2007).
[15] Chen, Y., Liu, Z., Zhang, Z., "Tensor-Based Human Body Modeling," Proceedings of the 2013 IEEE Conference on Computer Vision and Pattern Recognition, 105-112 (2013).
[16] Razevig, V. V., "Simulation of recording the microwave holograms of complex objects by the near range radars," Science and Education 6, 336-353 (2014) (in Russian).
[17] <http://www.autodesk.com/products/3ds-max/> (15 January 2015).
[18] Kuriksha, A. A., "The reciprocal projection algorithm used for reconstructing a spatial distribution of wave sources," Journal of Communications Technology and Electronics 47(12), 1355-1360 (2002).